

Accepted Manuscript

Composition Control of $\text{Cu}_2\text{ZnSnSe}_4$ -Based Solar Cells Grown by Coevaporation

H. Tampo, K. Makita, H. Komaki, A. Yamada, S. Furue, S. Ishizuka, H. Shibata, K. Matsubara, S. Niki

PII: S0040-6090(13)01934-2
DOI: doi: [10.1016/j.tsf.2013.11.078](https://doi.org/10.1016/j.tsf.2013.11.078)
Reference: TSF 32915

To appear in: *Thin Solid Films*

Received date: 30 November 2012
Revised date: 16 November 2013
Accepted date: 18 November 2013



Please cite this article as: H. Tampo, K. Makita, H. Komaki, A. Yamada, S. Furue, S. Ishizuka, H. Shibata, K. Matsubara, S. Niki, Composition Control of $\text{Cu}_2\text{ZnSnSe}_4$ -Based Solar Cells Grown by Coevaporation, *Thin Solid Films* (2013), doi: [10.1016/j.tsf.2013.11.078](https://doi.org/10.1016/j.tsf.2013.11.078)

This is a PDF file of an unedited manuscript that has been accepted for publication. As a service to our customers we are providing this early version of the manuscript. The manuscript will undergo copyediting, typesetting, and review of the resulting proof before it is published in its final form. Please note that during the production process errors may be discovered which could affect the content, and all legal disclaimers that apply to the journal pertain.

Composition Control of $\text{Cu}_2\text{ZnSnSe}_4$ -Based Solar Cells Grown by Coevaporation

H. Tampo*, K. Makita, H. Komaki, A. Yamada, S. Furue, S. Ishizuka, H. Shibata, K. Matsubara, and S. Niki

*National Institute of Advanced Industrial Science and Technology (AIST), Research Center for Photovoltaics
Technologies, Tsukuba, Ibaraki 305-8568, Japan*

Abstract:

The relationship between the composition and conversion efficiency of $\text{Cu}_2\text{ZnSnSe}_4$ (CZTSe)-based solar cells was investigated. CZTSe films were grown by thermal deposition using a coevaporation method. It was found that the composition of CZTSe and Na concentration [Na] have strong correlations to the conversion efficiency, and higher-efficiency samples were obtained with the composition ratios closer to $\text{Zn/Sn} \sim 1.6$, $\text{Cu}/(\text{Zn}+\text{Sn}) \sim 0.8$, and $[\text{Na}] \sim 2\%$. The highest conversion efficiency ($\eta = 2.1\%$) was obtained in the composition region, and the composition was significantly nonstoichiometric. The CZTSe composition was automatically fixed on a tie line between $\text{Cu}_2\text{ZnSnSe}_4$ and ZnSe , and it was demonstrated that this composition can be expressed by one parameter. The structural and electrical properties of the high- and low-efficiency samples were also investigated. No significant differences in such properties were observed between the high- and low-efficiency samples by surface, x-ray diffraction measurements, and Raman measurements. However, the low-efficiency sample showed a high carrier concentration.

Keywords: CZTSe, composition ratio, Na concentration, tie line, coevaporation

*Corresponding author: e-mail: tampo-21@aist.go.jp, phone: +81-29-861-9148

1. Introduction

$\text{Cu}_2\text{ZnSn}(\text{S},\text{Se})_4$ -based materials (CZTSSe) have recently been attracting much attention as next-generation solar cell materials because of the mass production of CuInGaSe_2 (CIGS) solar cells and demands of III-element-free chalcogenide semiconductors. Recently, several groups have reported the high conversion efficiency solar cells using CZTSSe- and $\text{Cu}_2\text{ZnSnS}_4$ -based materials (CZTS) [1-4]. In particular, the highest conversion efficiency ($\eta=11.1\%$) was achieved using CZTSSe absorption films [3, 4], which is an alloy of CZTS and CZTSe. However, there are few reports on S-free CZTSe-based solar cells and their basic properties [5-7] in spite of the many investigations of CZTS [1, 2, 8, 9]. CZTSSe is a member of $\text{I}_2\text{-II-IV-VI}_4$ compound semiconductors, and band gap energy is tunable by controlling the VI group ratio, that is $\text{Se}/(\text{Se}+\text{S})$ composition ratio; the band gap energy varies from 1.0 to 1.5 eV [10, 11]. CZTS is a sulfide compound and less toxic and abundant compared to a selenide compound of CZTSe. However, CZTSe which is a component of CZTSSe must be investigated because the highest conversion efficiency was obtained by CZTS-CZTSe alloy, CZTSSe. CZTS-based films were reported to be relatively easily synthesized with low cost, for example, by hydrazine-based and nanocrystal-based solutions [3, 4, 12], therefore, CZTSSe-based materials have a possibility to open up another fabrication method of solar cells.

In this study, we investigated CZTSe solar cells and characterized the structure and electrical properties of CZTSe, focusing on the relationship between the composition of CZTSe and the conversion efficiency of CZTSe solar cells. We grew CZTSe films by thermal evaporation based on molecular beam epitaxy (MBE) system, which enable precise control of supply elements.

2. Experimental Setup

CZTSe films were deposited by the thermal evaporation of elemental Cu, Zn, Sn, and Se all together, a type of coevaporation method. The growth setup in this study is MBE-based evaporation system described [13] except for replacing a liquid nitrogen cooling system in the growth chamber to a water cooling system. Growth temperature was fixed at 370°C , and the thickness of the CZTSe films was 2 μm , and the typical growth rate was $\sim 2 \mu\text{m/h}$. CZTSe solar cells were fabricated similarly to CIGS solar cells except for the use of an absorption film as follows: The substrate used was soda-lime glass (SLG). A Mo back electrode, a CZTSe film, a CdS film prepared by chemical bath deposition, an intrinsic ZnO (i-ZnO) film, and a transparent conducting oxide (TCO) film were successively deposited to yield TCO/i-ZnO/CdS/CZTSe/Mo/SLG. ZnO-based TCOs were deposited by rf sputtering method. The thicknesses of the Mo electrode, CdS film, i-ZnO film, and TCO film were 800 nm, 50 nm, 50 nm, and 500 nm, respectively. The structural properties of CZTSe films were characterized by scanning electron microscopy (SEM) measurements, x-ray diffraction (XRD) measurements, and Raman measurements. SEM measurements were operated at an electron beam acceleration of 5 kV (Hitachi S-4800II). XRD measurements were carried out using PANalytical X'pert MRD system with a Cu rotating anode as a x-ray source and parallel beam geometry. Raman spectra were measured using a Reinshaw inVia Raman microprobe with 532 nm laser excitation. The composition of the CZTSe films was estimated by electron probe microanalysis (EPMA), and an acceleration voltage of 7 kV was used, which corresponds to an effective estimated depth of 200 nm. Electrical properties were evaluated by current density-voltage (J - V) and capacitance-voltage (C - V) measurements. The photovoltaic parameters of the solar cells were measured under AM 1.5 G (100 mW/cm^2) illumination at

25°C.

3. Results and Discussion

3.1 Relationship between composition of CZTSe and conversion efficiency of CZTSe solar cells

Fig. 1 shows the relationship between composition of CZTSe films and conversion efficiency of CZTSe solar cells. The Se content of CZTSe was almost 50% ($\pm 2\%$), therefore, the Zn/Sn and Cu/(Zn+Sn) ratios can fully cover the composition range of CZTSe. The colors indicate the efficiency of the solar cells. A conversion efficiency of 2.1% was obtained as the highest in this study. As shown in the figure, the high-efficiency samples obtained were significantly nonstoichiometric and had Zn/Sn=1.6 and Cu/(Zn+Sn)=0.8. CZTS solar cells have been reported to use high-efficiency samples that were largely nonstoichiometric (Zn/Sn=1.25 and Cu/(Zn+Sn)=0.85) [1, 14]. However, the relationship between the efficiency and composition of CZTSe seems to be weak. As shown in Fig. 1, the compositions of CZTSe are distributed on a line, and high- and low-efficiency samples coexist for similar compositions. We discuss this as follows.

Fig. 2 shows a triangular plot of the composition of CZTSe films, and the triangular apexes consist of CuSe, ZnSe, and SnSe. Note that Se content is fixed at 50% in the triangular plot, which was confirmed from the experimental results explained in the previous paragraph. A triangular plot of Cu₂Se-ZnSe-SnSe₂ is often used because formal valencies of Cu, Zn, and Sn were +1, +2, and +4, respectively. However in this study, the Se composition was always 50at%, and in order to express 50% in the plot, we used the triangular plot of CuSe-ZnSe-SnSe. As shown in the figure, all the samples were closely distributed on the line of ZnSe and Cu₂ZnSnSe₄. In this study, CZTSe composition was controlled by adjusting the Cu, Zn, and Sn beam fluxes, which were individually changed (a much higher Se flux was always used). That is, the composition ratios of the film were significantly shifted from the supply ratios, and the compositions were automatically fixed on the line. Note that the composition of CZTSe films toward thickness direction was evaluated by secondary ion mass spectroscopy (SIMS), and the depth profile was found to be almost flat for Cu, Zn, Sn, and Se compositions without Na concentration. All the CZTSe films in this study showed a single-phase nature without other compounds as shown by the result of XRD and Raman measurements as follows, however, the structure could not be strictly determined by these two measurements; they are discussed following section. The single-phase region was much wider than the reported phase diagram [15]; however, the origin of this was not clear yet. The composition on the line can be expressed as Cu_{2x}ZnSn_xSe_(1+3x), and this expression is used in the following section, where x denotes the partition ratio of ZnSe and Cu₂ZnSnSe₄. Note that the single-phase region might extend from Cu₂ZnSnSe₄ to Cu₂SnSe₃. However, we could not conclude the extension due to lack of data in this study.

It was found that Na concentration [Na] has a significant effect on the efficiency of CZTSe cells. As discussed above and as shown in Fig. 1, the high- and low-efficiency samples coexist at close compositions, and other factors that change the efficiency are suggested from the result. Fig. 3 shows the efficiency as functions of CZTSe composition and [Na]. As shown in Fig. 2, CZTSe was grown on the specific line, so we can express the composition by one parameter by projecting the actual composition to the specific line. The parameter is the thermo equilibrium line projected parameter (TP) defined as,

$$TP = ([Sn]/[Zn] + [Cu]/2[Zn])/2,$$

where [Sn], [Zn], and [Cu] are the atomic concentrations of Sn, Zn, and Cu, respectively. The first term indicates

the projection to the line connecting ZnSe and $\text{Cu}_2\text{ZnSnSe}_4$ from the actual composition point started from Cu vertex in the triangular plot, and the second term is the projection to the line from the actual composition point started from Sn vertex. TP is their mean. TP corresponds to x if the composition of CZTSe can be expressed as $\text{Cu}_{2x}\text{ZnSn}_x\text{Se}_{(1+3x)}$. As shown in Fig. 3, a strong [Na] effect on the efficiency was observed as well as a TP effect, which is the composition effect. The high-efficiency samples showed [Na]~2%. The Na effect was also well investigated for CIGS [16, 17]. The source of Na is considered from soda-lime glass. Na concentration varied with same growth conditions and same CZTSe compositions, that is, Na concentration in CZTSe was not controllable; the difference might be due to different SLG production lot. However more detailed investigation is necessary in a further study.

The photovoltaic properties of the CZTSe solar cells with the highest efficiency $\eta=2.1\%$ in this study are shown in Fig. 4 and Fig. 5. Fig. 4 shows the J - V curve. The cell efficiency was 2.1 % with an open circuit voltage (V_{OC}) of 0.355 V, a short circuit current density (J_{SC}) of 9.75 mA/cm^2 , and a fill factor of 0.604 (an active area of 0.515 cm^2). J_{SC} is considerably low compared with that of a typical CuInSe_2 cell with a similar band gap energy $E_g \sim 1.0$ eV, whose reported efficiency was over 36 mA/cm^2 [18]. Moreover, the J_{SC} of the CZTS cell with $E_g \sim 1.5$ eV was 17.9 mA/cm^2 [1], and the J_{SC} of the CZTSe cells in this study was considered low. The low J_{SC} was consistent with the external quantum efficiency (EQE) curve shown in Fig. 5. The maximum EQE was 0.3; it significantly dropped from 600 nm toward the longer-wavelength region.

In order to obtain a higher efficiency, higher-temperature growth is considered necessary because the higher-efficiency samples for CZTSe were obtained using higher-thermal treatments at over 500°C such as post deposition annealing or multi-stage growth using a Cu_xSe_y phase [6, 7]. However, for single-stage coevaporation at over 400°C we could not control the composition owing to the strong Sn and Se re-evaporation under a normal growth condition [19]. Therefore, another growth technique at higher temperatures such as those used for these thermal treatments is expected to result in a higher efficiency.

3.2 Relationship between film properties of CZTSe and cell efficiency

In this section, we discuss the relationship between the film properties of CZTSe and cell efficiency. As discussed above, particularly in Fig. 3, the composition of CZTSe and [Na] affected cell efficiency. We also showed similarities and differences in film properties between high- and low-efficiency samples. In this study, we investigated the structural and electrical properties shown in Table. I. We selected samples with various cell efficiencies.

As shown in Fig. 6, no significant differences were observed from the SEM measurements of the samples with various efficiencies. The grains of CZTSe films in this study were smaller than that of reported CZTS and CZTSSe, which ranged from 500 nm to 1 μm [1-4]. The smaller grain size is considered to be due to the use of lower growth temperature of 370°C in this study. The larger grain size was reported in the case of a higher annealing temperature of the CZTSe films from 255°C to 400°C [20]. Also, the larger the grain size, the higher the growth temperature, was also observed in CZTS [21]. However, a higher growth temperature was reported to lead to CZTSe decomposition, particularly, by the re-evaporation of Sn and Se [19], and it is considered not so easy to use high growth temperatures. The smaller grain size might lead to the low J_{SC} , but more precise study of this is necessary.

XRD patterns also showed no significant differences between the high- and low-efficiency samples in Fig. 7. As shown in the figure, all peaks were assigned to CZTSe compound and Mo, and no other phases were observed; the peak intensity ratios were almost identical for all the samples. It was also found that the samples had a preferential (112) orientation and their lattice constants were estimated as $a=0.568$ nm, and $c=1.137$ nm under the assumption of $c=2a$; these values are similar to those previously reported [22].

Moreover, we could not observe any differences among the Raman measurements shown in Fig. 8. The spectra show clear CZTSe peaks at 172, 192, and 230 cm^{-1} , which values are almost identical reported [23,24]. We can see a small peak at approximately around 370 cm^{-1} ; however, the origin of this peak, which is not ZnSe (205, 251 cm^{-1}) or Cu_2Se (260 cm^{-1}), was unclear. Note that the peak at approximately around 370 cm^{-1} was also reported in Ref. 20 and 21; they were also not assigned to particular components. From the structural evaluations by XRD, and Raman measurement, we concluded two things: First, the CZTSe films used in this study are all single phases. This conclusion is also supported by flat depth profiles of the composition evaluated by SIMS measurements, the result of which is not shown here. Second, there are no significant differences between the high- and low-efficiency samples.

In this study, the structure of CZTSe films was unknown, kesterite, stannite, or other structures. That is, we could not distinguish these structures by mean of these experimental results. For $\text{I}_2\text{-II-IV-VI}_4$ compounds such as $\text{Cu}_2\text{ZnSnSe}_4$, $\text{Cu}_2\text{ZnSnS}_4$ and so on, two main tetragonal structure types are known: the kesterite and stannite structure; it is difficult to distinguish these structures and also difficult to confirm their coexistence [25]. Therefore neutron diffraction measurement or/and x-ray absorption fine structure analysis have been conducted to distinguish the structure.

Differences were observed in the capacitance-voltage (C - V) measurement as shown in Fig. 9. The C - V method is easily applicable to solar cells because C - V measurements can be carried out using the same configuration of J - V measurement with only the measurement equipments being different. The carrier profiles were estimated by the standard analysis method [26]. From the figures, the carrier concentration of cell A with the highest efficiency showed a carrier concentration of $\sim 3 \times 10^{17} \text{ cm}^{-3}$; those of cells B and C were similar. However, cells D and E with the lowest efficiency showed a higher carrier concentration about $\sim 6 \times 10^{17} \text{ cm}^{-3}$. A higher carrier concentration of an absorption layer leads to a thinner depletion layer, which means a decrease in effective absorption area for standard p-n junction solar cells [26]. Therefore, a high carrier concentration is one of the important causes of low efficiency. The carrier concentration of cell A is much higher than those of conventional CIGS films, which are reported to range from a high of 10^{15} to a low of 10^{16} cm^{-3} [27]. Therefore, in order to obtain higher-efficiency CZTSe based cells, the carrier concentration should be reduced, and a method of such reduction should be investigated. The $\text{Cu}/(\text{Zn}+\text{Sn})$ ratio of CZTSe was reported to affect carrier concentration [24] and carrier concentration is considered to strongly correlate with the composition of CZTSe and [Na] as shown in Fig. 3. The effects of Na in CZTSe-based materials have not been reported, but we could speculate the effect based on CIGS-based materials. For CIGS-based materials, hole concentration is reported to increase with increasing Na concentration [17]. It is concluded in Ref. that Na causes the compensation of Se vacancy by oxygen incorporation. Note that Se vacancy plays as a donor, therefore, decrease of Se vacancy leads to increase of hole concentration. The similar phenomenon by Na incorporation in CZTSe might occur, however, more detailed investigation is necessary.

4. Conclusions

The composition of CZTSe and [Na] were found to strongly affect the conversion efficiency of CZTSe solar cells and high-efficiency samples showed TP~0.6 and [Na]~2%, which were significantly nonstoichiometric; the highest conversion efficiency was 2.1%. The composition of CZTSe was found to be automatically fixed on the tie line between $\text{Cu}_2\text{ZnSnSe}_4$ and ZnSe, and the composition was demonstrated to be expressed by one parameter i.e., TP. There were no significant differences in structural measurements between the low- and high-efficiency samples; however, the low-efficiency samples showed higher carrier concentrations.

Acknowledgement

This work was partially supported by the Japan Science and Technology Agency (JST) as part of the Core Research for Evolution Science and Technology Program (CREST).

References

- [1] H. Katagiri, K. Jimbo, S. Yamada, T. Kamimura, W.S. Maw, T. Fukano, T. Ito, T. Motohiro, *Appl. Phys. Express*, 1 (2008) 041201.
- [2] K. Wang, O. Gunawan, T. Todorov, B. Shin, S.J. Chey, N.A. Bojarczuk, D. Mitzi, S. Guha, *Appl. Phys. Lett.*, 97 (2010) 143508.
- [3] D.A.R. Barkhouse, O. Gunawan, T. Gokmen, T.K. Todorov, D.B. Mitzi, *Prog. Photovolt: Res. Appl.*, 20 (2012) 6-11.
- [4] K. Todorov, J. Tang, S. Bag, O. Gunawan, T. Gokmen, Y. Zhu, D.B. Mitzi, *Adv. Energy Mat.*, 3 (2013) 34-38.
- [5] G. Zoppi, I. Forbes, R.W. Miles, P.J. Dale, J.J. Scragg, L.M. Peter, *Prog. Photovolt: Res. Appl.*, 17 (2009) 315-319.
- [6] B. Shin, Y. Zhu, N.A. Bojarczuk, S. Jay Chey, S. Guha, *Appl. Phys. Lett.*, 101 (2012) 053903.
- [7] I. Repins, C. Beall, N. Vora, C. DeHart, D. Kuciauskas, P. Dippo, B. To, J. Mann, W.-C. Hsu, A. Goodrich, R. Noufi, *Solar Energy Materials and Solar Cells*, 101 (2012) 154-159.
- [8] H. Katagiri, K. Jimbo, W.S. Maw, K. Oishi, M. Yamazaki, H. Araki, A. Takeuchi, *Development of CZTS-based thin film solar cells*, *Thin Solid Films*, 517 (2009) 2455-2460.
- [9] B.-A. Schubert, B. Marsen, S. Cinque, T. Unold, R. Klenk, S. Schorr, H.-W. Schock, *Progress in Photovoltaics: Research and Applications*, 19 (2011) 93-96.
- [10] J. Krustok, R. Josepson, T. Raadik, M. Danilson, *Physica B*, 405 (2010) 3186.
- [11] K. Ito, T. Nakazawa, *Jpn. J. Appl. Phys.*, 27 (1988) 2094.
- [12] Q. Guo, G. M. Ford, W.-C. Yang, B. C. Walker, E. A. Stach, H. W. Hillhouse, R. Agrawal, *J. Am. Chem. Soc.* 131 (2009) 11672.
- [13] K. Sakurai, A. Yamada, P. Fons, K. Matsubara, T. Kojima, S.Niki, T. Baba, N. Tsuchimochi, Y. Kimura, H. Nakanishi, *J. Phys. Chem. Solids*, 64 (2003) 1877.
- [14] H. Katagiri K. Jimbo, M. Tahara, H. Araki, K. Oishi, *Mater. Res. Soc. Symp. Proc.* 1165(2009) M04-01
- [15] I.V. Dudchak, L.V. Piskach, *J. Alloys and Compounds*, 351 (2003) 145-150.

- [16] D. Rudmann, A.F. da Cunha, M. Kaelin, F. Kurdesau, H. Zogg, A.N. Tiwari, G. Bilger, Appl. Phys. Lett., 84 (2004) 1129.
- [17] S. Ishizuka, A. Yamada, M.M. Islam, H. Shibata, P. Fons, T. Sakurai, K. Akimoto, S. Niki, J. Appl. Phys., 106 (2009) 034908.
- [18] For example, A.M. Gabor, J.R. Tuttle, D.S. Albin, M.A. Contreras, R. Noufi, A.M. Hermann, Appl. Phys. Lett., 65 (1994) 198.
- [19] A. Redinger, S. Siebentritt, Appl. Phys. Lett., 97 (2010) 092111.
- [20] P.M.P. Salomé, P.A. Fernandes, A.F. da Cunha, Thin Solid Films, 517 (2009) 2531-2534.
- [21] T. Tanaka, D. Kawasaki, M. Nishio, Q. Guo, H. Ogawa, Phys. Stat. Solidi (c), 3 (2006) 2844-2847.
- [22] H. Matsushita, T. Maeda, A. Katsui, T. Takizawa, J. Cryst. Growth, 208 (2000) 416-422.
- [23] M. Altosaar, J. Raudoja, K. Timmo, M. Danilson, M. Grossberg, J. Krustok, E. Melikov, Phys. Stat. Solidi (a), 205 (2008) 167-170.
- [24] T. Tanaka, T. Sueishi, K. Saito, Q. Guo, M. Nishio, K.M. Yu, W. Walukiewicz, J. Appl. Phys., 111 (2012) 053522.
- [25] S. Schorr, Solar Energy Materials and Solar Cells 95 (2011) 1482.
- [26] For example, S.M. Sze, "Physics of Semiconductor devices", 3rd Ed, WILEY, 2.2 depletion region, p80
- [27] For example, D.L. Young, J. Keane, A. Duda, J.A.M. AbuShama, C.L. Perkins, M. Romero, R. Noufi, Progress in Photovoltaics: Research and Applications, 11 (2003) 535-541.,

Figure captions

- Fig. 1 Relationship between composition of CZTSe and efficiency of CZTSe cell. The cross point of $Zn/Sn=1$ and $Cu/(Zn+Sn)=1$ shows the stoichiometry point of $Cu_2ZnSnSe_4$. The colors indicate the efficiency.
- Fig. 2 Triangle plot of CZTSe. The plot consists of three components i.e., CuSe, ZnSe and SnSe; Se composition is fixed at 50% in the entire area of the plot.
- Fig. 3 Efficiency as functions of TP and [Na]. The colors indicate the efficiency as in Fig. 1.
- Fig. 4 $J-V$ curve for highest-efficiency sample.
- Fig. 5 External quantum efficiency as a function of wavelength for the same sample in Fig. 4.
- Fig. 6 Surface observation by SEM for samples in Table I. The colors of the frames indicate the efficiency as in Fig. 1.
- Fig. 7 X-ray diffraction curve for samples in Table I. The colors of the curves indicate the efficiency as in Fig. 1.
- Fig. 8 Raman spectra of samples in Table I. The colors of the spectra indicate the efficiency as in Fig. 1.
- Fig. 9 Carrier profiles estimated by $C-V$ measurement for samples in Table I. The colors of the profiles indicate the efficiency as in Fig. 1.

Table 1

Sample compositions and Na concentrations for various characterizations.

Figure 1

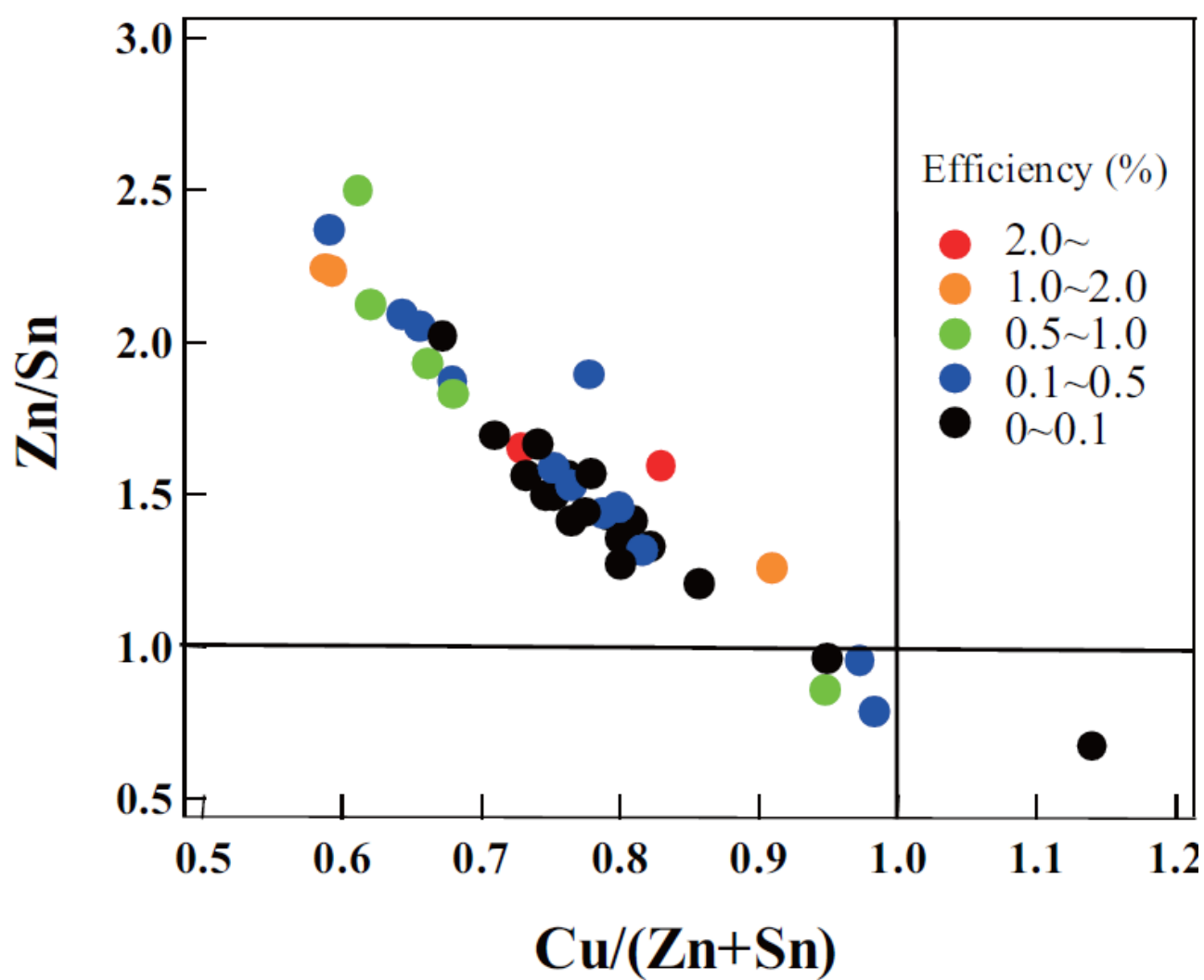


Figure 2

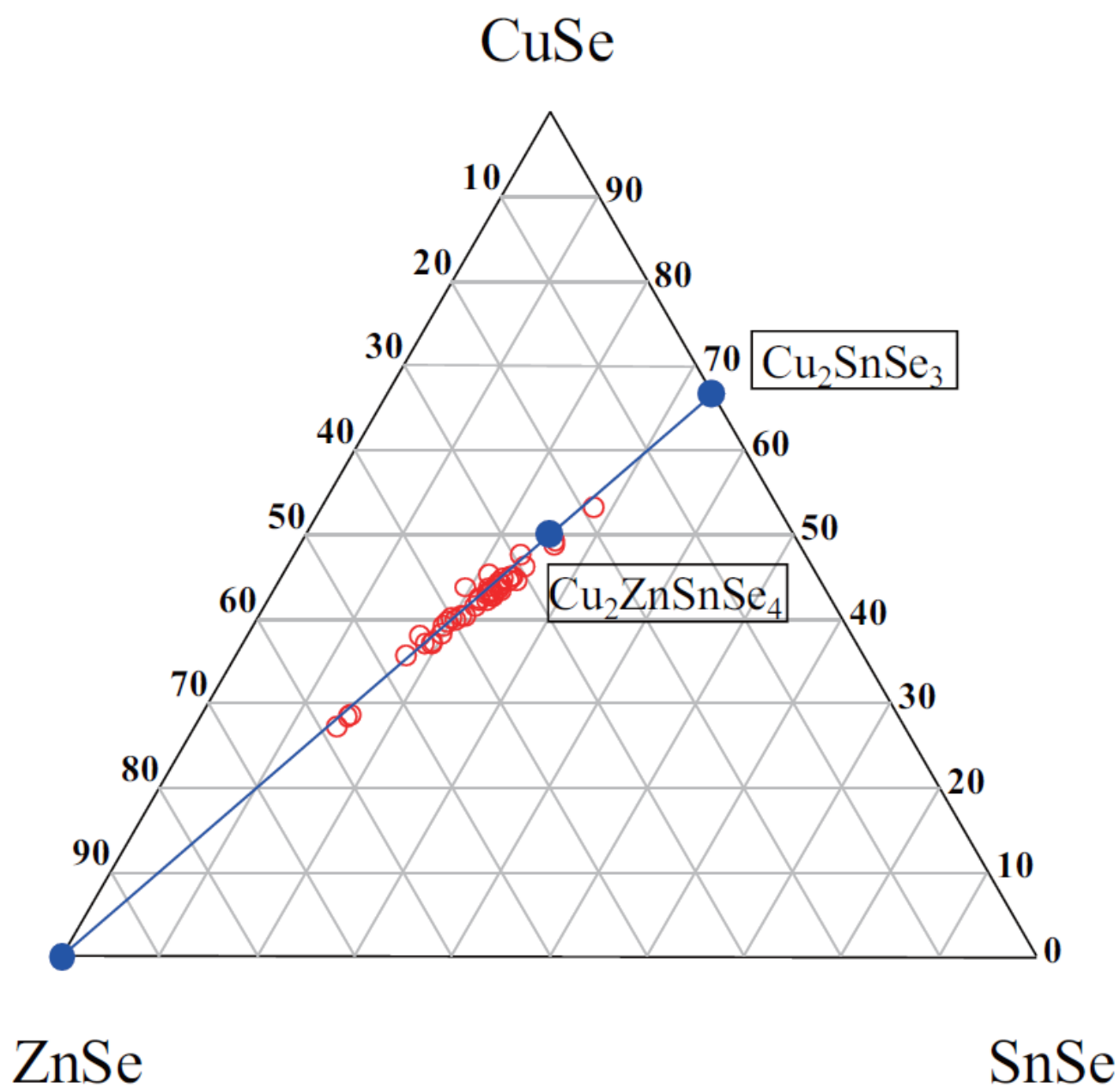


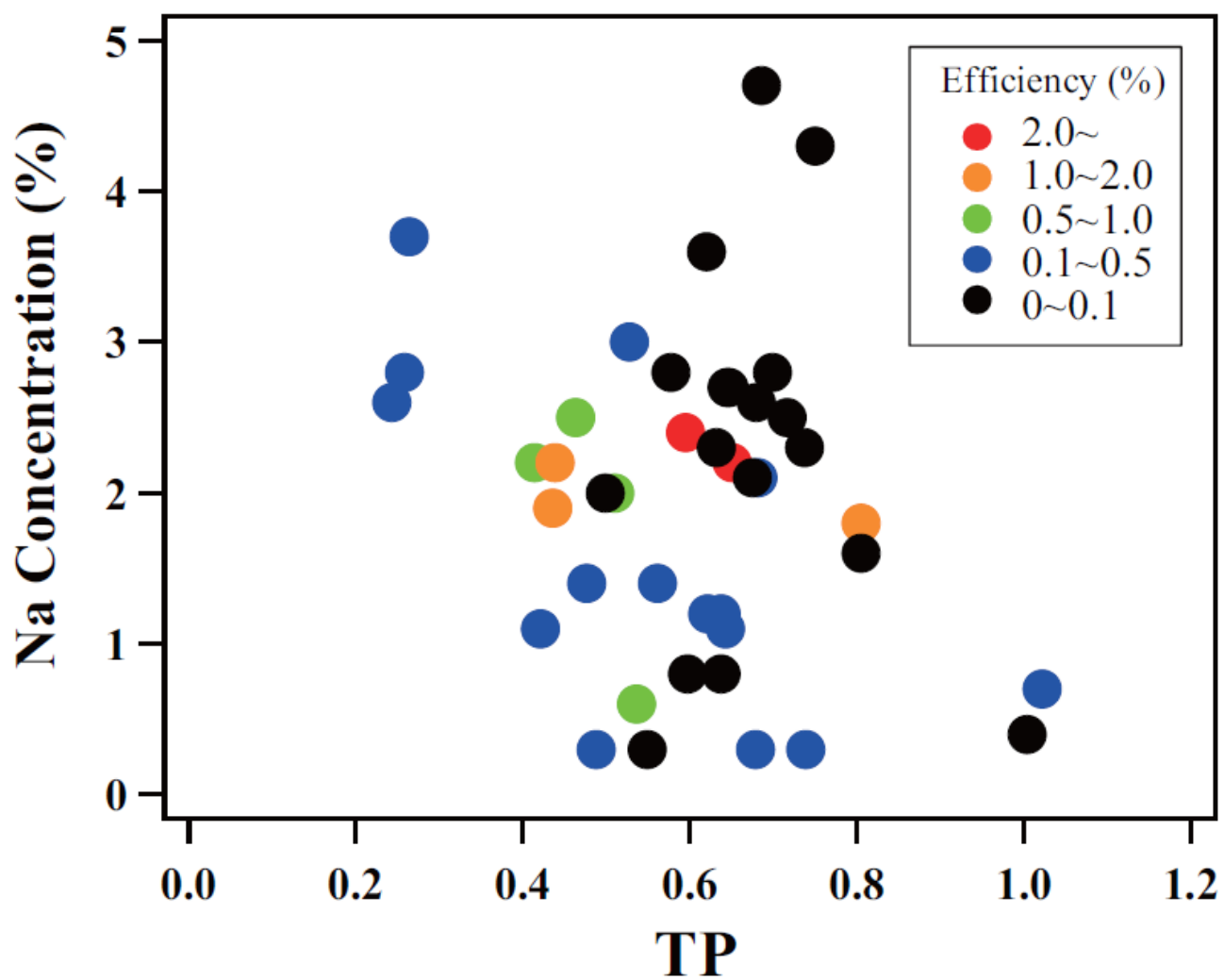
Figure 3

Figure 4

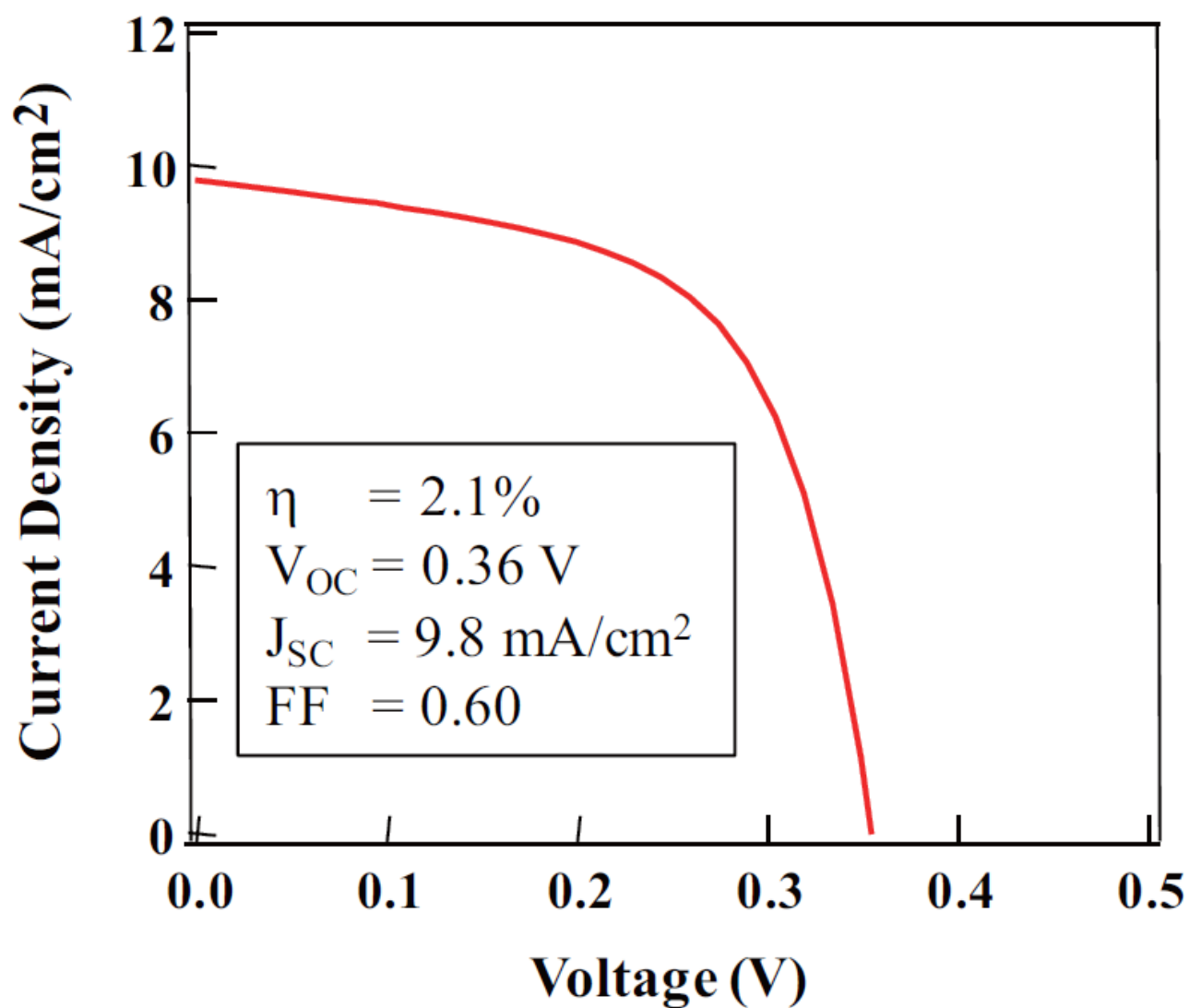


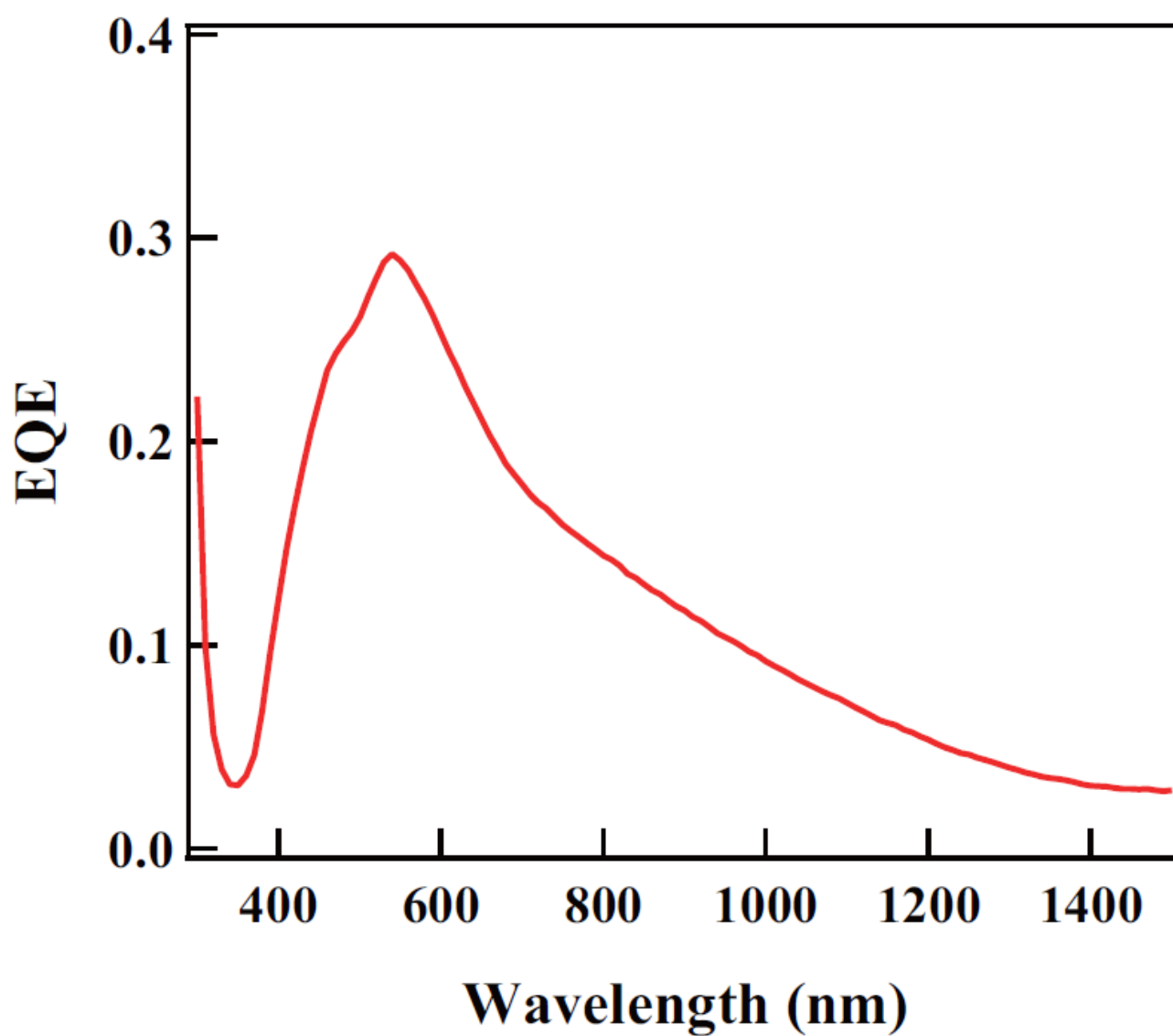
Figure 5

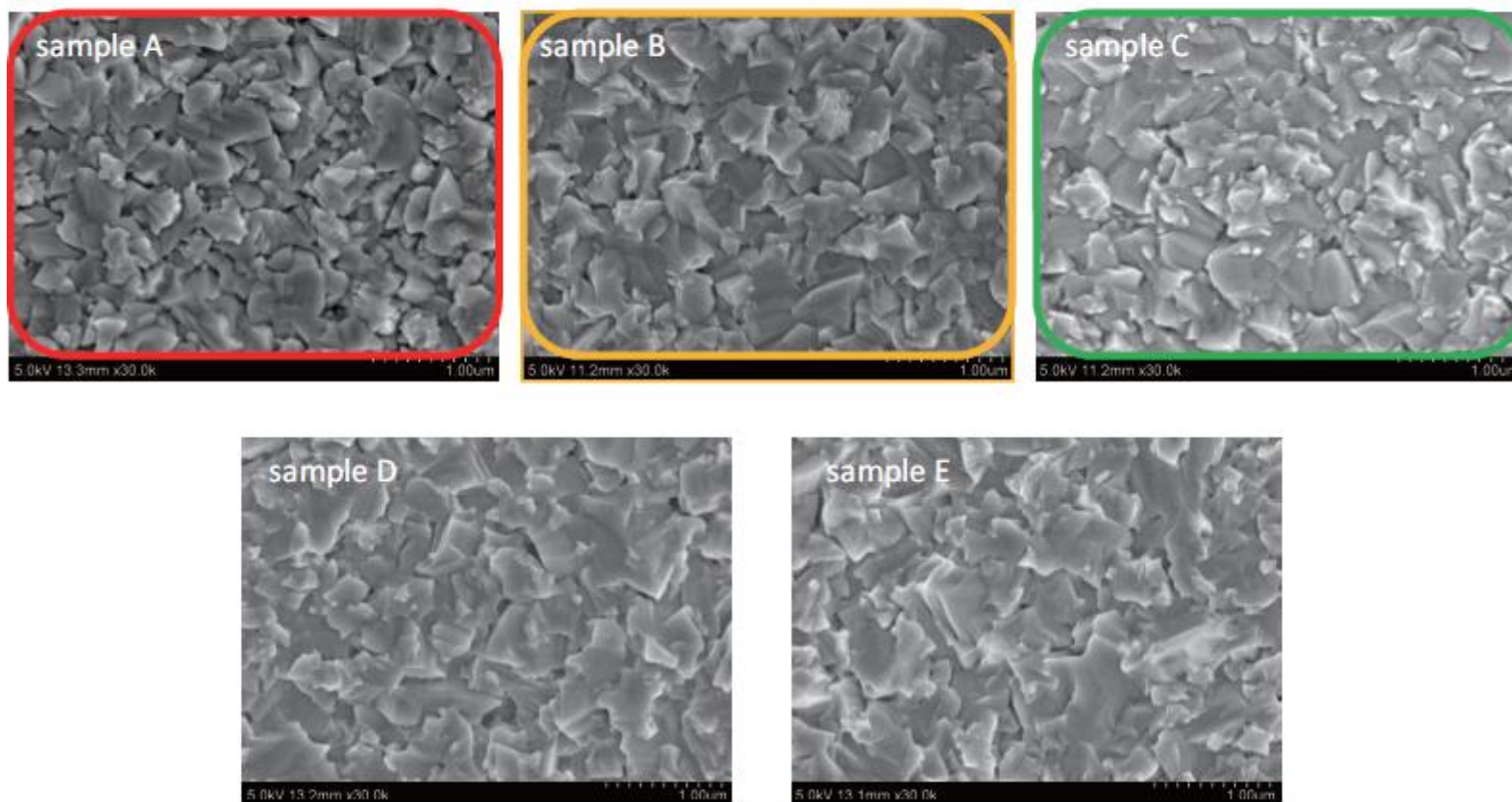
Figure 6

Figure 7

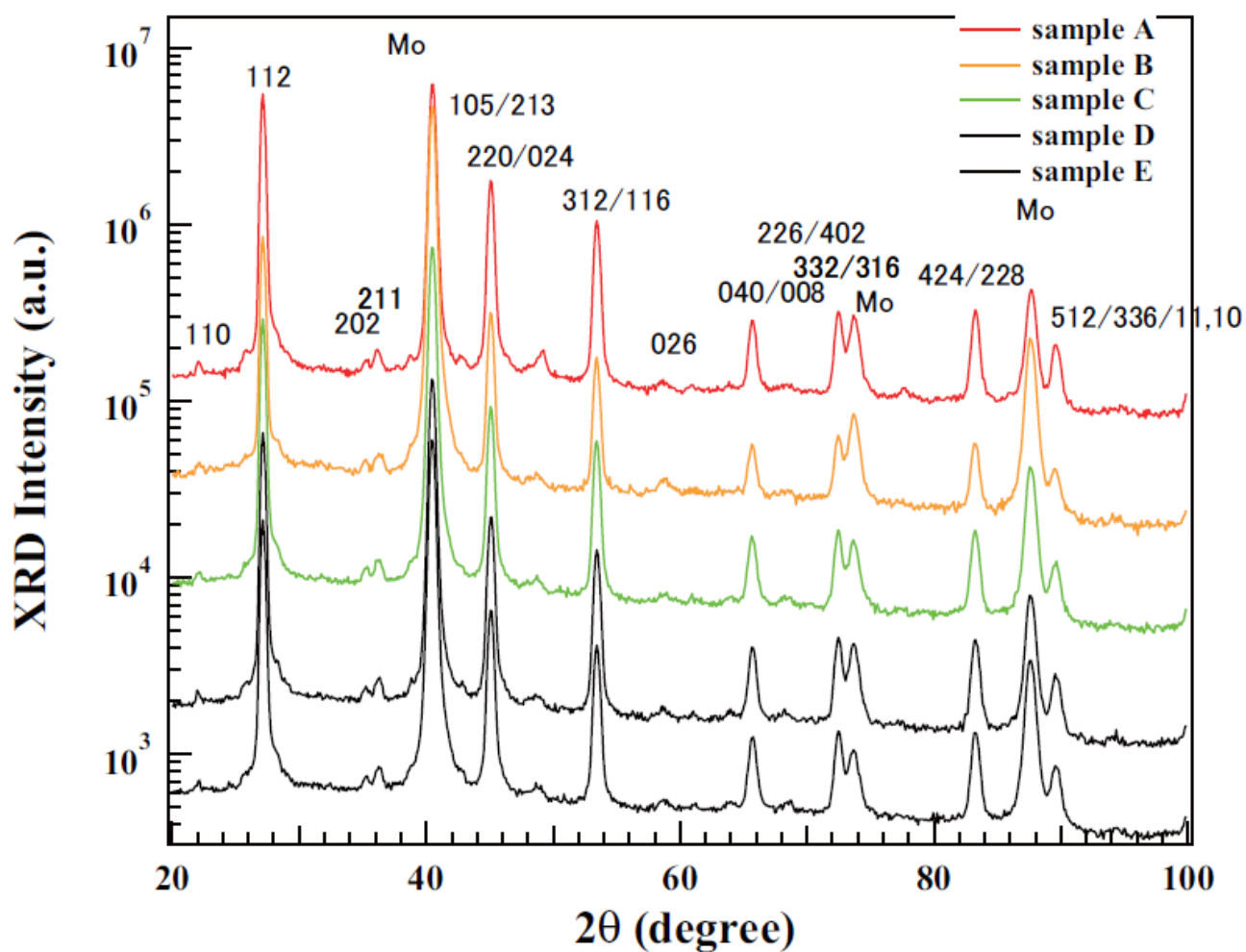


Figure 8

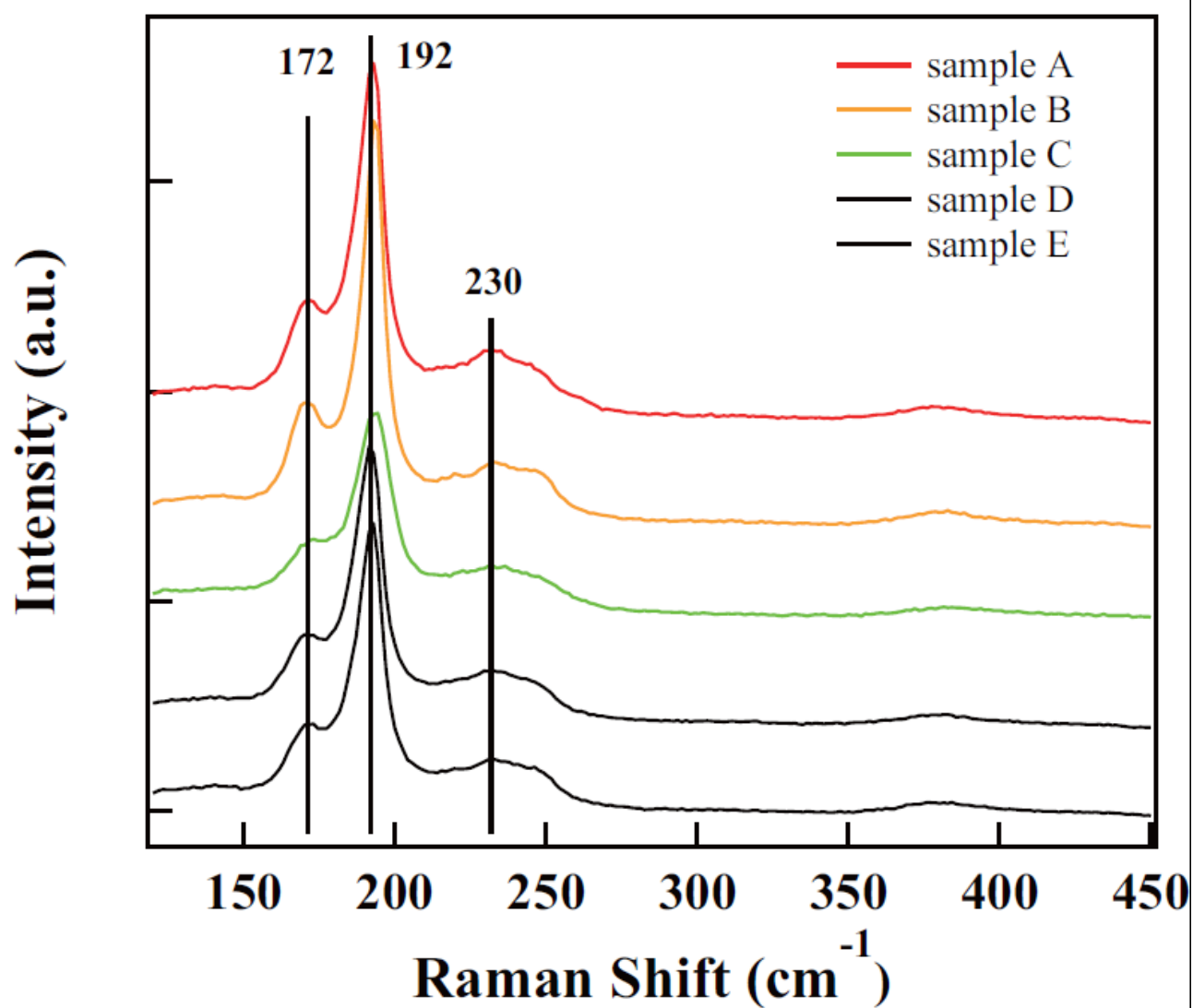


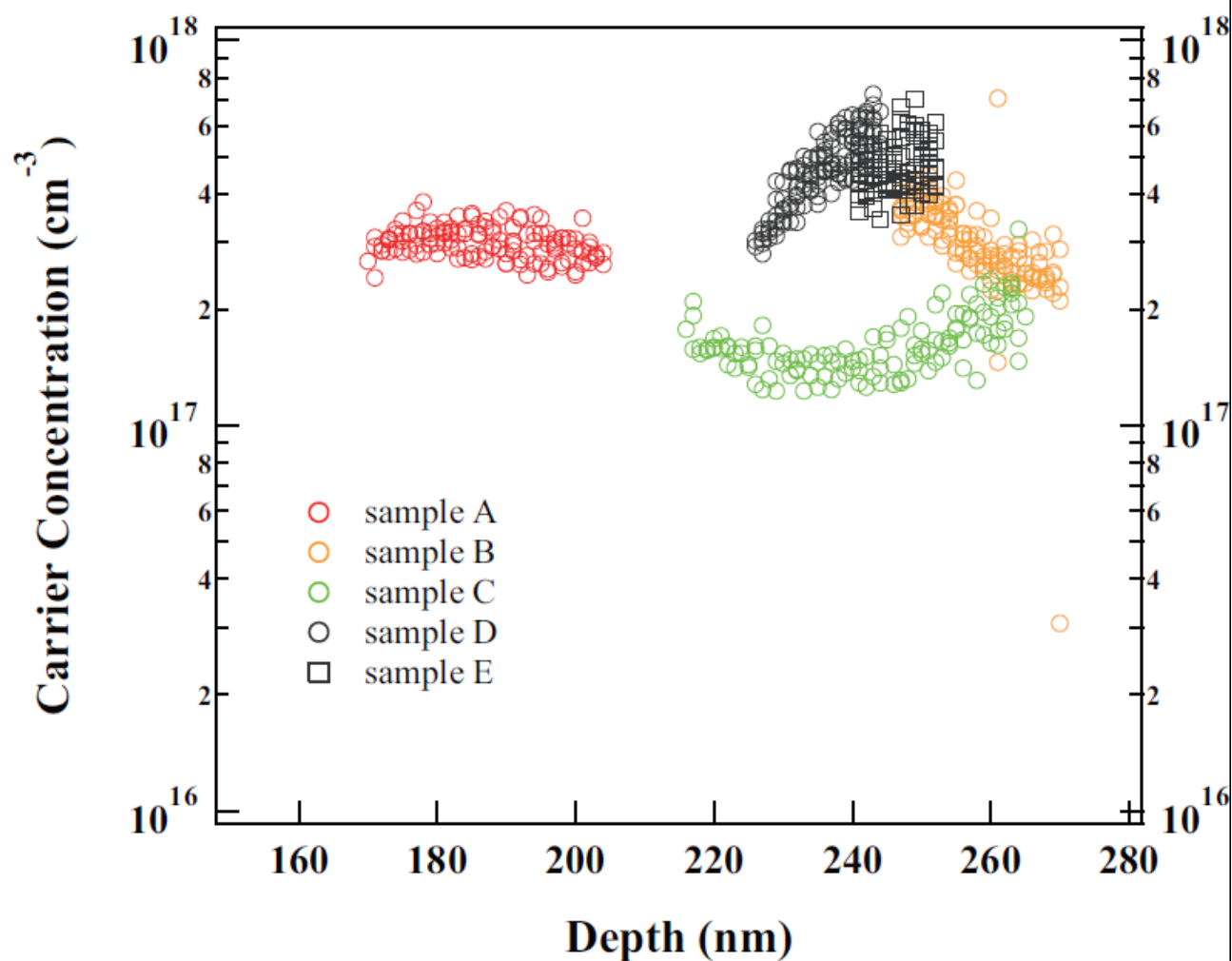
Figure 9

Table 1

	Cu/(Zn+Sn)	Zn/Sn	TP	[Na] (%)	Efficiency (%)
sample A	0.83	1.60	0.65	2.2	2.0
sample B	0.91	1.26	0.80	1.8	1.7
sample C	0.61	2.50	0.41	2.2	0.6
sample D	0.71	1.70	0.58	2.8	0.05
sample E	0.73	1.56	0.62	3.6	0.05

Highlights

$\text{Cu}_2\text{ZnSnSe}_4$ (CZTSe).

The CZTSe composition and Na concentration strongly affected efficiency of CZTSe.

The composition of CZTSe was automatically determined on a special tie line.

There were no structural differences between high- and low-efficiency samples.

Low-efficiency samples showed a higher carrier concentration.